Available online at www.sciencedirect.com
SCIENCE DIRECT®
Journal of the European Ceramic Society 25 (2005) 3207–3212
www.elsevier.com/locate/jeurceramsoc

Lanthanum and nitrogen co-doped $SrTiO_3$ powders as visible light sensitive photocatalyst

Jinshu Wang[a,b,*], Shu Yin[a], Masakazu Komatsu[a], Tsugio Sato[a]

[a] *Division of Advanced System, Institute of Multidisciplinary Research for Advanced Materials, Tohoku University, Sendai 980-8577, Japan*
[b] *School of Materials Science and Engineering, Beijing University of Technology, Beijing 100022, China*

Received 6 May 2004; received in revised form 13 July 2004; accepted 20 July 2004
Available online 13 October 2004

Abstract

Lanthanum and nitrogen co-doped $SrTiO_3$ was prepared by a mechanochemical reaction method using $SrTiO_3$, urea and La_2O_3 as the raw materials. Nitrogen-doped $SrTiO_3$ could be prepared by heating the mixture of $SrTiO_3$ and La_2O_3 under flowing NH_3 gas at 600 °C. The sample prepared with 0.2 mol% La_2O_3, 22 mol% urea and 77.8 mol% $SrTiO_3$ which has nearly the same nitrogen and lanthanum doping atomic fractions could be obtained by a mechanochemical method and exhibited high photocatalytic activities. Under the irradiation of light with wavelengths larger than 400 and 290 nm, the photocatalytic activity of nitrogen and lanthanum co-doped $SrTiO_3$ was 2.6 and two times greater than that of pure $SrTiO_3$. A new absorption edge, which was formed in the visible light region and higher visible light absorption after co-doping were the reason for the high visible light photocatalytic activity of this substance.

Keywords: Titanates; Milling; Optical properties; Doping; Functional applications; $SrTiO_3$; Photocatalysis

1. Introduction

Strontium titanate ($SrTiO_3$) is an important material which has applications in photocatalysis and electronics industry and has attracted much attention from both fundamental and practical viewpoints.[1–3] Its photocatalytic properties in UV light range have been investigated in the past. The redox potential of electrons and holes induced by UV irradiation is powerful enough to decompose hazardous pollutants into nontoxic substances[4,5] and to cleave H_2O into H_2 and O_2 gas.[6] However, UV light is less than 5% of the sunlight on the earth. Visible light photoactivity has been introduced into TiO_2 by doping with transition metals[7] and nonmetallic elements.[8–12] It was reported that Cr or V ion-implanted TiO_2 absorbed visible light efficiently and could decompose NO by visible light irradiation. However, it seems that anion doping is more efficient for improving the photocatalytic activity. Among all the anion-doped photocatalysts, nitrogen doping has aroused great attention since Asahi et al. claimed the narrowing of the band gap of TiO_2 by doping with nonmetallic atoms and actually showed the visible light responsive photocatalytic activity of nitrogen-doped TiO_2.[8] We also found that nitrogen doping is also effective to add visible light responsive photocatalytic activity to $SrTiO_3$.[13] It is suspected, however, that replacing O^{2-} with N^{3-} would result in the formation of anion defects for the charge compensation and the anion defects would act as electron–hole recombination centers. It is expected that the charge compensation is satisfied if O^{2-} is replaced with N^{3-} together with replacing Sr^{2+} or Ti^{4+} with a higher valence metal ion. It is known that La^{3+} has nearly the same ionic radius (0.115 nm) as Sr^{2+} (0.113 nm) and can replace Sr^{2+} in $SrTiO_3$ without producing a large lattice strain. In a previous paper, we have successfully doped nitrogen in $SrTiO_3$ lattice by mechanochemical reactions.[13] It was also reported that heat treatment of titania in ammonia gas atmosphere was effective for doping nitrogen.[8,9] Therefore, in the present study, nitrogen and lanthanum co-doped $SrTiO_3$ was synthesized by both mechanochemical reaction and heat treatment in ammonia gas, and the visible

* Corresponding author. Tel.: +86-10-67391101; fax: +86-10-67392840.
E-mail address: wangjsh@bjpu.edu.cn (J. Wang).

0955-2219/$ – see front matter © 2004 Elsevier Ltd. All rights reserved.
doi:10.1016/j.jeurceramsoc.2004.07.027

light responsive photocatalytic activity of the samples was evaluated.

2. Experimental

2.1. Sample preparation

Stoichiometric strontium titanate was synthesized by solid state reaction of $SrCO_3$ and TiO_2 (Kanto Chem. Co. Inc. Japan) at 1100 °C for 2 h as shown in Eq. (1)

$$SrCO_3 + TiO_2 \rightarrow SrTiO_3 + CO_2 \quad (1)$$

$(NH_2)_2CO$ and La_2O_3 (Kanto Chem. Co. Inc. Japan) powders were used as doping sources. The samples were prepared as follows. Sample 1 (heating method): 1 g of the mixed powder of 77.8 mol% $SrTiO_3$, 22.0 mol% $(NH_2)_2CO$ and 0.2 mol% La_2O_3 was put into an Al_2O_3 crucible and heated at 600 °C under flowing NH_3 gas for 3 h. Samples 2–5 (mechanochemical reaction method): Three grams of the mixed powders of 77.9, 77.8, 77.7, and 76.0 mol% $SrTiO_3$, 22.0 mol% $(NH_2)_2CO$ and 0.1, 0.2, 0.3, 2.0 mol% La_2O_3 were charged in a zirconia pot of 45 cm^3 volume with seven zirconia balls of 15 mm in diameter and ball-milled for 2 h at room temperature and 700 rpm rotation speed using a planetary ball mill (Pulverisette-7, Fritsch, Germany), respectively. Then, the ground powders were calcined at 400 °C to remove remaining urea and by-products such as $NH_2CONHCONH_2$, $C_3H_3N_3O_3$, etc.

2.2. Catalyst characterization

X-ray diffraction (XRD) patterns were obtained using a Shimadzu XD-D1 diffractometer using graphite monochromatized Cu Kα radiation. Crystallite size was calculated from the line broadening of corresponding X-ray diffraction peaks according to the Warren and Averbach equation:[14]

$$D = \frac{\lambda 180}{\pi \cos \theta L} \quad (2)$$

where L is the line width at medium height, λ the wavelength of the X-ray radiation (0.15418 nm) and θ the diffraction angle. The particle size and shape were evaluated by transmission electron microscopy (JEM-2000EX). Specific surface areas (BET), Barrett–Joyner–Halenda (BJH) pore size distributions and pore parameters of the powder samples were determined by nitrogen adsorption–desorption isotherm measurements at 77 K (Quantachrome NOVA 1000-TS). The binding energies of Sr, Ti, N, La and O were measured at room temperature using an electron spectrometer (Perkin-Elmer PHI 5600). The peak positions of each element were corrected by using that of C1s (284.6 eV). The amount of nitrogen and oxygen in the $SrTiO_3$ was determined by an oxygen–nitrogen analyzer (HORIBA, EMGA-2800) and the sensitivity of the nitrogen measurement was about 0.00001 wt.% (0.1 ppm).

2.3. Photocatalytic activity measurement

A 450 W high pressure mercury arc was used as the light source, where the light wavelength was controlled by selecting filters, i.e., Pyrex glass for cutting off the light of $\lambda <$ 290 nm, Kenko L41 Super Pro (W) filter <400 nm. The photocatalyst sample was placed in a hollow place of 20 mm × 15 mm × 0.5 mm on a glass holder plate and set in the center of the reactor. The elimination of nitrogen monoxide was determined by measuring the concentration of NO gas at the outlet of the reactor (373 cm^3) during the photoirradiation under a constant flow of 1 ppm NO and 50 vol.% air (balance N_2) mixed gas (200 $cm^3\ min^{-1}$). The gas contained 0.157 wt.% NO, 23.474 wt.% O_2 and 76.369 wt.% N_2. The concentration of NO was determined by a NO_x analyzer (Yanaco, ECL-88A).

3. Results and discussions

3.1. Characterization of the samples

Fig. 1 shows the XRD patterns of samples 1 and 3 made by heating and mechanochemical reaction, respectively. All of the samples consisted of single phase $SrTiO_3$ which is completely identified as a perovskite-type structure having cubic symmetry. In addition, the X-ray diffraction patterns of the milled sample exhibited broadening of the crystalline peaks. The result calculated by Eq. (2) showed that the sample made by the mechanochemical reaction had a crystallite size of 20.2 nm. The specific surface areas of these samples together with the starting $SrTiO_3$ are shown in Table 1. After heat treatment under NH_3 flow, the specific surface area of $SrTiO_3$ decreased from 4.1 to 3.2 $m^2\ g^{-1}$. On the other hand, the samples prepared by mechanochemical reaction showed much higher specific surface areas around 22.7–25.1 $m^2\ g^{-1}$. Direct TEM observation showed that doped $SrTiO_3$ prepared by the heating method consisted of relatively large particles of about 0.2–0.4 μm in diameter (see Fig. 2a). On the other hand, the sample made by mechanochemical reaction consisted of spherical particles of two different sizes, i.e., tiny particles of

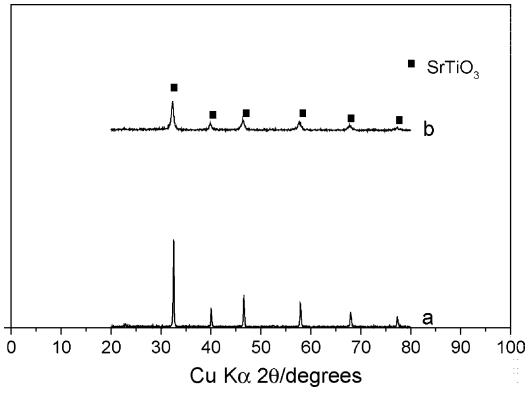

Fig. 1. XRD pattern of (a) Sample 1 and (b) Sample 3.

Table 1
Initial compositions, doping fraction of nitrogen and lanthanum and specific surface areas of the samples prepared

Samples	Preparation method	Initial composition (mol%)			N (wt.%)	x and y in $La_xSr_{1-x}TiO_{3-y}N_y$			Specific surface area ($m^2\ g^{-1}$)
		$SrTiO_3$	$(NH_2)_2CO$	La_2O_3		x_1	x_2	y	
$SrTiO_3$		100				0	0	0	4.1
1	Calcination	77.8	22.0	0.2	0.100	0.0051	0	0.0131	3.2
2	Mechanochemical	77.9	22.0	0.1	0.149	0.0026	–	0.0195	24.5
3	Mechanochemical	77.8	22.0	0.2	0.165	0.0051	0.0162	0.0216	23.4
4	Mechanochemical	77.7	22.0	0.3	0.188	0.0077	–	0.0247	22.7
5	Mechanochemical	76.0	22.0	2	0.214	0.0526	0.1272	0.0284	25.1

x_1: calculated from the initial amount of lanthanum in the raw material; x_2: calculated from XPS data.

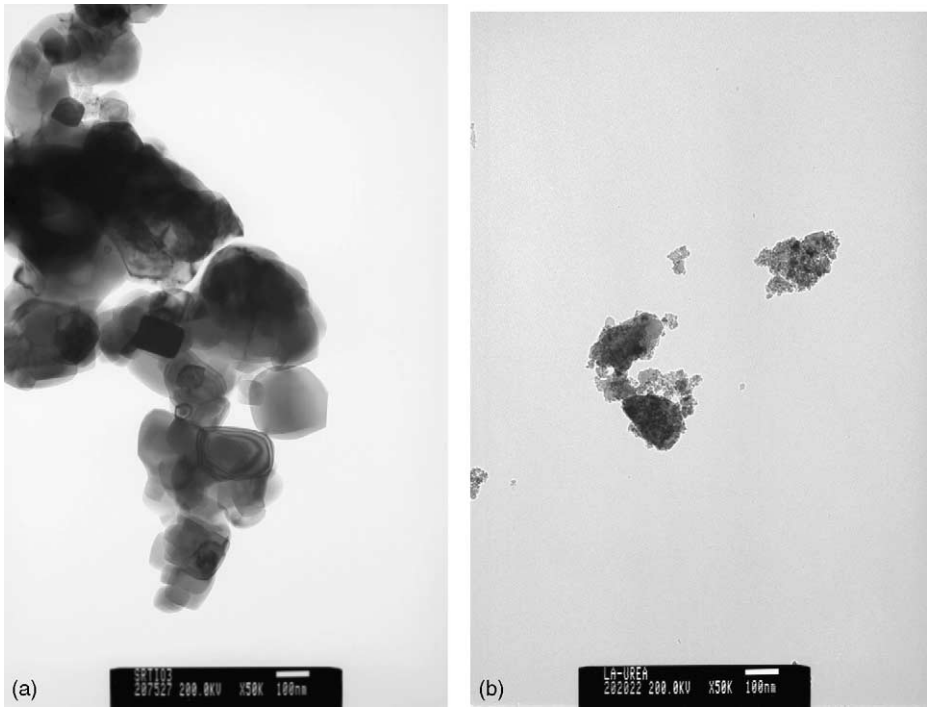

Fig. 2. Transmission electron micrographs of (a) Sample 1 and (b) Sample 3.

ca. 20 nm and large agglomerated particles of 100–200 nm in diameter (Fig. 2b). The size of 20 nm was similar to that calculated by XRD. The larger particles were covered with tiny crystallites. The tiny particles seemed to be caused by high energy grinding. During high energy milling, $SrTiO_3$ powders were subjected to severe mechanical deformation by the collisions with milling balls and pot. Consequently, plastic deformation at high strain rates occurred within $SrTiO_3$ powders and the average grain size could be reduced to about 20 nm.

In order to check whether nitrogen and lanthanum have been incorporated successfully into the $SrTiO_3$ lattice, X-ray photoelectron spectra analysis was carried out. Fig. 3 shows N1 XPS spectra of different samples. Samples prepared by mechanochemical reaction or heating both show N1s peak at about 398.4 eV. It may be attributed to the doping state of nitrogen, since the binding energy of N1s of urea used as a starting material for mechanochemical reaction is located at 1.3 eV higher energy (399.7 eV).

The shape of the La3d peak changed depending on the preparation method. The La3d spectra of La oxide consist of two doublets. The energy loss peaks appearing on the higher energy side of the 3d5/2 and 3d3/2 peaks in Fig. 4c are

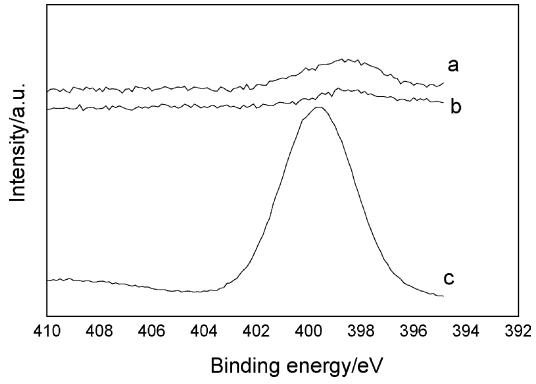

Fig. 3. XPS spectrum of N1s of (a) Sample 3, (b) Sample 1 and (c) urea.

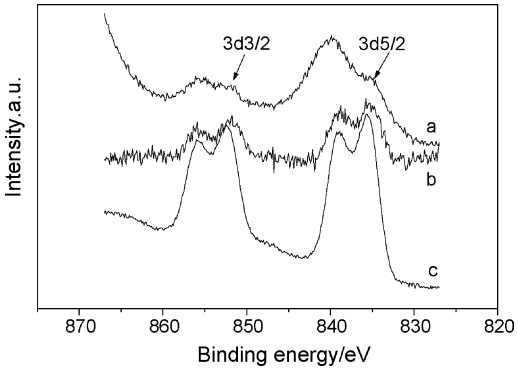

Fig. 4. XPS spectrum of La3d of (a) Sample 3, (b) Sample 1 and (c) pure La_2O_3.

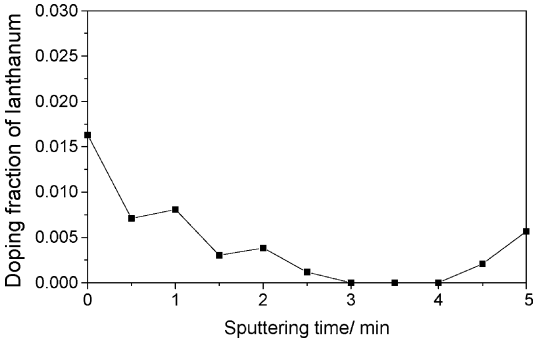

Fig. 5. Doping atomic fraction profile of lanthanum with sputtering time.

called satellite peaks. These peaks are believed to result from core–hole screening by nearly degenerate O2p and empty La 4f states. The general explanation for high binding energy satellite peaks of lanthanum oxide is that there is a charge transfer from O2p to the empty 4f state of La leading to the $3d^9 4f^1$ final state.[15] Compared with the La3d peak of pure La_2O_3 (Fig. 4c), the peak shape of the sample prepared by mechanochemical reaction method greatly changed (Fig. 4a). The most obvious change after doping was the decrease of the La3d core level intensity and the increase of the satellite peak intensity in the La3d doublet, indicating that the binding between lanthanum and oxygen changed. On the other hand, the sample prepared by the heating method exhibited a La3d peak shape similar to pure La_2O_3 (see Fig. 4b and c), indicating that La existed as La_2O_3 state and was not incorporated into $SrTiO_3$. Therefore, it may be concluded that the mechanochemical reaction method is efficient for co-doping of nitrogen and lanthanum in the $SrTiO_3$ lattice whereas the heating method at 600 °C could only be used for doping nitrogen. Doping lanthanum in the $SrTiO_3$ lattice includes breaking of the La–O bond, diffusion of lanthanum ions and the substitution reaction between La^{3+} and Sr^{2+} ions. It seems that heat treatment at 600 °C could not provide enough energy to break the La–O bonds. On the other hand, the mechanical stress provided by high energy ball-milling induced the destruction of La–O bonds and the formation of new bonds.

As stated above, La^{3+} has nearly the same ionic radius (0.115 nm) as Sr^{2+} (0.113 nm), so we could deduce that lanthanum and nitrogen ions substituted for strontium and oxygen ions, respectively, and the doped compound could be written as $La_xSr_{1-x}TiO_{3-y}N_y$. The concentrations of nitrogen in samples 1–5 were measured by an oxygen–nitrogen analyzer and those of lanthanum were calculated from both the initial content in the raw material and the XPS peak areas of individual elements through sensitivity factors for these elements provided by Perkin-Elmer PHI 5600 software. For the sample prepared with $SrTiO_3$, 22.0 mol% urea and 0.2 mol% La_2O_3, the atomic ratio of La/Sr was calculated as 0.0165, indicating the formation of $La_xSr_{1-x}TiO_{3-y}N_y$ with $x = 0.0162$ under the condition that lanthanum has a substitutional fraction of $f_s = 1$. It is reasonable to take the substitutional fraction as one based on the solubility rules for substitutional solid solutions. For the substitutional solid solutions, the extent of the substitution is mainly determined by the ionic size. The ionic radius of La^{3+} is close to that of Sr^{2+}, and the difference in the radii of these two ions is only 1.7%, far lower than the radii difference limit of 15% for the formation of substitutional solid solution.[16] The doping fractions of nitrogen and lanthanum of the various samples are summarized in Table 1. It is clear that the amount of doped lanthanum measured by the XPS method is higher than the initial concentration in the raw material. XPS is a surface analysis method and the concentration of lanthanum in Table 1 suggests that the lanthanum concentration near the powder surface is higher than that inside. Fig. 5 shows the doping atomic fraction profile of lanthanum with sputtering time. It indicates that in the initial stage, the doping fraction of lanthanum decreased with prolonging of sputtering time, in other words, decreased with the increase of depth. When the sputtering time is in the range 3–4 min, the doping fraction is zero. Further prolonging the sputtering time, the doping fraction of lanthanum increased, indicating that after being sputtered for 3.5 min, the site might be the center of the particles. Incorporating lanthanum into the $SrTiO_3$ lattice includes breaking of the La–O bond, diffusion of lanthanum ions and the substitution reaction between La^{3+} and Sr^{2+} ions. It seems that the incorporating reaction is relatively difficult to take place in the inner part of the particles. Since catalytic activities are highly surface-dependent, the lanthanum concentration near the powder surface determined by XPS influences catalyst activity greatly.

Taking urea as the nitrogen source, the following two reactions might take place during grinding:

$$2(NH_2)_2CO \rightarrow NH_3 + NH_2CONHCONH_2 \text{ (biuret)} \quad (3a)$$

$$3(NH_2)_2CO \rightarrow 3NH_3 + C_3H_3N_3O_3 \text{ (cyanuric acid)} \quad (3b)$$

Since two solid phases, biuret and cyanuric acid, have strong N–H and C–N bonds, it is difficult to react with $SrTiO_3$. NH_3 gas produced by these two reactions is easily absorbed on the surface of $SrTiO_3$ particles and react with $SrTiO_3$ to dope nitrogen. The solid-state interdiffusion reaction during reactive ball-milling was triggered by fragmentation of the $SrTiO_3$ powder thus creating new surfaces. These freshly created surfaces reacted with NH_3 and La_2O_3 to form

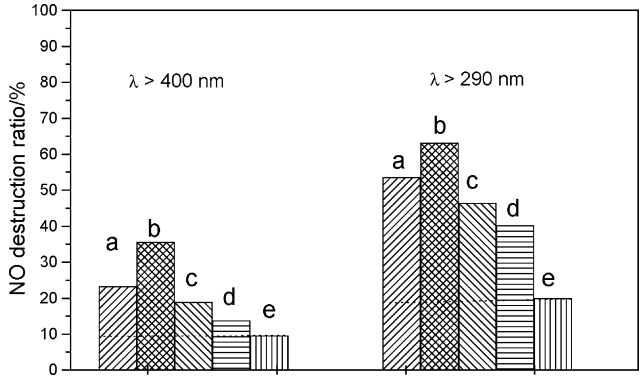

Fig. 6. The photocatalytic activity of various samples under visible light (λ > 400 nm) and ultraviolet light (λ > 290 nm): (a) Sample 1, (b) Sample 3, (c) Sample 3 before calcination, (d) $SrTiO_3$ and (e) blank without sample.

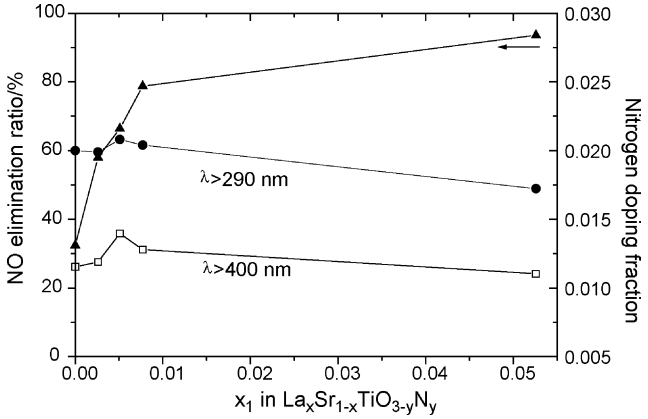

Fig. 7. The photocatalytic activity of samples 1–5 as a function of La^{3+} doping.

a nitrogen and lanthanum co-doped $SrTiO_3$ surface layer over the unreacted core particles. With further milling this doping reaction continued and a $La_xSr_{1-x}TiO_{3-y}N_y$ phase was formed resulting in a nanostructured nitrogen and lanthanum co-doped $SrTiO_3$.

3.2. Optical properties and photocatalytic activity for NO destruction

Fig. 6 shows the photocatalytic activity of undoped $SrTiO_3$, nitrogen-doped $SrTiO_3$ (Sample 1) and nitrogen and lanthanum co-doped $SrTiO_3$ (Sample 3) for the NO elimination under irradiation of visible light (λ > 400 nm) and UV light (λ > 290 nm). It took about 10 min to reach the steady state after light irradiation. It was also found that when the light was turned off, NO concentration returned to its initial level of 1 ppm within 10 min. These results suggested that the light energy is essential for the oxidation of NO, i.e., NO was photocatalytically eliminated. The oxidation degrees by blank test without photocatalyst were 9.6 and 20% under the irradiation of light with wavelength λ > 400 and 290 nm, respectively (Fig. 6e). As expected from its large band gap energy, undoped $SrTiO_3$ exhibited little photocatalytic activity, whereas samples 1 and 3 showed higher photocatalytic activity under visible light irradiation (λ > 400 nm). It is seen that Sample 3 showed the highest NO destruction ability under visible light irradiation, i.e., 35.8% NO could be destructed, which is about 2.6 and 1.4 times larger than that by pure $SrTiO_3$ and Sample 1, respectively (Fig. 6a, b and d). Furthermore, the co-doped $SrTiO_3$ sample had good photocatalytic activity in the near ultraviolet light range also, i.e., 63.2% NO could be destructed which was about two times higher than that of pure $SrTiO_3$. On the other hand, the nitrogen and lanthanum co-doped $SrTiO_3$ sample without calcination had lower capability for the elimination of NO. It might be due to the inhibition of NO adsorption by remaining by-products such as NH_3, $NH_2CONHCONH_2$, $C_3H_3N_3O_3$, etc. and unreacted $(NH_2)_2CO$. Heat treatment of the sample at appropriate temperature such as 400 °C might remove these unfavorable contaminations and also decrease the number of defects in the lattice of $SrTiO_3$ produced during high energy grinding because of the high recovery rate of the lattice defects at elevated temperature.

The photocatalytic activity and the doping fraction of nitrogen as function of the doping fraction of lanthanum, x_1, determined from the initial composition of the sample are shown in Fig. 7. The NO elimination ratio of the samples increased with the increase of doping fraction of lanthanum up to $x_1 = 0.005$, then decreased with the further increase of the lanthanum content. The increase in the initial stage may be due to the increase in nitrogen content. On the other hand, the decrease of the photocatalytic activity with excess lanthanum doping may be due to the formation of a cation defect and/or Ti^{3+} for the charge compensation. For the Sample 5 made with 2 mol% La_2O_3–22 mol% $(NH_2)_2CO$–$SrTiO_3$, the lanthanum doping content near the particle surface reached 0.1272 whereas the nitrogen doping content is only 0.0284 (see Table 1), indicating that the nitrogen doping content could not increase so much due to the relatively big difference of ionic size of N^{3-} ($r = 0.171$ nm) and O^{2-} ($r = 0.140$ nm) although the extent of substitution of La^{3+} to Sr^{2+} could be very high. Excess La^{3+} doping will lead to the formation of cation defects and/or reduction of Ti^{4+} to Ti^{3+} which will decrease the photocatalytic activity of the sample because of a decrease in the thickness of the space-charge layer as deep Ti^{3+} traps are populated.[17] Therefore, an appropriate doping fraction of lanthanum which is consistent with that of nitrogen doping could efficiently improve the photoreactivity of the sample.

It is well-known that the photocatalytic activity of a semiconductor is related to its band gap structure. The diffuse reflectance spectra of pure $SrTiO_3$, nitrogen-doped $SrTiO_3$ (Sample 1), lanthanum and nitrogen co-doped $SrTiO_3$ (Sample 3) and the sample prepared by high energy milling of a mixture of $SrTiO_3$ and 2 mol% La_2O_3 are represented in Fig. 8. Pure $SrTiO_3$ shows an absorption edge at 390 nm corresponding to the band gap energy of 3.18 eV (see Fig. 8d). The co-doped samples have two absorption edges at 390 and

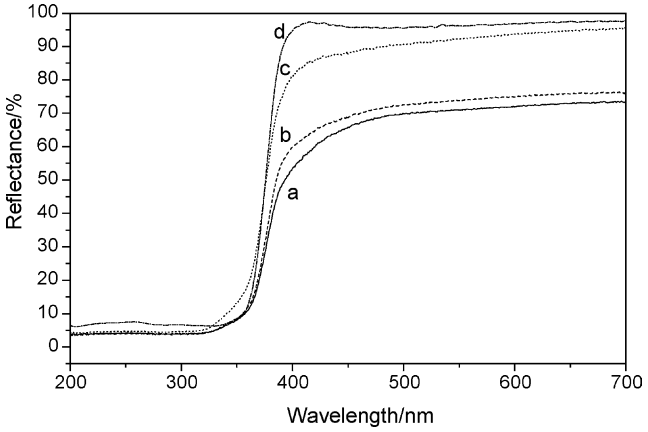

Fig. 8. The diffuse reflection spectra of (a) Sample 3, (b) Sample 1, (c) ground mixture of 2 mol% La_2O_3 and $SrTiO_3$ and (d) pure $SrTiO_3$.

450 nm. These absorption edges may be attributed to those of $SrTiO_3$ and nitrogen-doped $SrTiO_3$ lattice, respectively, since the ground mixture of $SrTiO_3$ and La_2O_3 exhibited only one absorption edge at 390 nm (see Fig. 8c). Fig. 8 and Table 1 suggest that lanthanum doping could increase the nitrogen doping content. Nitrogen doping could generate the absorption edge in the visible light range and result in the improvement of NO photo-oxidation ability under visible light irradiation. The photocatalytic activity results indicate that co-doping of lanthanum and nitrogen in $SrTiO_3$ could generate a stable visible light responsive photocatalyst with good NO elimination potential.

4. Conclusions

(1) Mechanochemical synthesis provides an efficient method for co-doping of nitrogen and lanthanum in the $SrTiO_3$ lattice by using $(NH_2)_2CO$ and La_2O_3 as the nitrogen and lanthanum sources. The co-doped sample could not be obtained by heating a mixture of $SrTiO_3$ and La_2O_3 under flowing NH_3.
(2) The content of doped nitrogen increased with the amount of lanthanum. The sample which has nearly the same lanthanum and nitrogen doping fraction exhibited high photocatalytic activity.
(3) The lanthanum and nitrogen co-doped $SrTiO_3$ has a band gap absorption edge at about 450 nm and functions as a visible light responsive photocatalyst for the elimination of nitrogen monoxide.

References

1. Yukawa, H., Nakatsuka, K. and Morinaga, M., Electronic structures of hydrogen in perovskite-type oxide $SrTiO_3$. *Solid State Ion.*, 1999, **116**, 89–98.
2. Domen, K., Kudo, A. and Onishi, T., Mechanism of photocatalytic decomposition of water into H_2 and O_2 over NiO-$SrTiO_3$. *J. Catal.*, 1986, **102**, 92–96.
3. Astala, R. and Bristowe, P. D., Ab initio and classical simulations of defects in $SrTiO_3$. *Comp. Mat. Sci.*, 2001, **22**, 81–86.
4. Ahuja, S. and Kutty, T. R. N., Nanoparticles of $SrTiO_3$ prepared by gel to crystallite conversion and their photocatalytic activity in the mineralization of phenol. *J. Photochem. Photobiol. A: Chem.*, 1996, **97**, 99–107.
5. Li, Q. S., Domen, K., Naito, S., Onishi, T. and Tamaru, K., Photocatalytic synthesis and photo-decomposition of ammonia over $SrTiO_3$ and $BaTiO_3$ based catalysts. *Chem. Lett.*, 1983, **3**, 321–324.
6. Domen, K., Naito, S. and Onishi, T., Photocatalytic decomposition of liquid water on a NiO $SrTiO_3$ catalyst. *Chem. Phys. Lett.*, 1982, **92**(4), 433–434.
7. Takeuchi, M., Yamashita, H., Matsuoka, M., Anpo, M., Hirao, T., Itoh, N. *et al.*, Photocatalytic decomposition of NO under visible light irradiation on the Cr-ion-implanted TiO_2 thin film photocatalyst. *Catal. Lett.*, 2000, **67**, 135–137.
8. Asahi, R., Morikawa, T., Ohwaki, T., Aoki, K. and Taga, Y., Visible-light photocatalysis in nitrogen-doped titanium oxides. *Science*, 2001, **293**, 269–271.
9. Irie, H., Watanabe, Y. and Hashimoto, K., Nitrogen-concentration dependence on photocatalytic activity of $TiO_{2-x}N_x$ powders. *J. Phys. Chem. B.*, 2002, **106**, 5029–5033.
10. Umebayashi, T., Yamaki, T., Tanaka, S. and Asai, K., Visible light-induced degradation of methylene blue on S-doped TiO_2. *Chem. Lett.*, 2003, **4**, 330–331.
11. Khan, S. U. M., Al-Shahry, M. and Ingler Jr., W. B., Efficient photochemical water splitting by a chemically modified *n*-TiO_2. *Science*, 2002, **297**, 2243–2246.
12. Irie, H., Watanabe, Y. and Hashimoto, K., Carbon-doped anatase TiO_2 powders as a visible-light sensitive photocatalyst. *Chem. Lett.*, 2003, **12**, 1156–1157.
13. Wang, J., Yin, S., Komatsu, M., Zhang, Q., Saito, F. and Sato, T., Mechanochemical synthesis and photocatalytic activity of nitrogen doped $SrTiO_3$. *J. Ceram. Soc. Jpn.*, 2004, **5**, S1408–S1410.
14. Colon, G., Hidalgo, M. C., Macias, M., Navio, J. A. and Dona, J. M., Influence of residual carbon on the photocatalytic activity of TiO_2/C samples for phenol oxidation. *Appl. Catal. B: Environ.*, 2003, **43**, 163–173.
15. Wang, J., Wu, W. and Feng, D., *Introduction to XPS/XAES/UPS.* National Defense Press, Beijing, 1992.
16. Ding, Z., Wang, M., Pan, S., Lin, Y., Wang, M., Wang, Y. *et al.*, *Physical Chemistry of Silicates*. Chinese Architecture Press, Beijing, 1987.
17. Torimoto, T., Fox, R. J. and Fox, M. A., *J. Electrochem. Soc.*, 1996, **11**, 3712–3717.